



Porosity gradients as a means of driving lateral flows at cometary surfaces

Chariton Christou^{a,b,*}, S. Kokou Dadzie^b, Raphael Marschall^{c,d}, Nicolas Thomas^c

^a Tickmill Group, EC2Y 9DT, London, UK

^b Heriot-Watt University, Institute of Mechanical Process and Energy Engineering, EH14 4AS, Edinburgh, Scotland, UK

^c Physikalisches Institut, University of Bern, Switzerland

^d International Space Science Institute, Hallerstrasse 6, CH-3012, Bern, Switzerland

ABSTRACT

The Rosetta spacecraft has provided invaluable and unexpected information about cometary outgassing. The on-board instruments ROSINA, MIRO, and VIRTIS showed non-uniform outgassing of H₂O over the surface of the nucleus. Rarefied gas flows display remarkable flow phenomena that may help explain diverse physical observations and models have been used in various engineering applications. Typical examples are flows generated by temperature variations such as thermal creeping flows that may have applications in cometary research. In this paper, we demonstrate how porosity variations in a porous medium combined with rarefaction can also lead to high tangential speed flow at a surface. Outgassing through a porous surface layer has been postulated as one possible mechanism at the cometary surfaces. We use the Direct Simulation Monte Carlo (DSMC) method to investigate such flows. The porous media structure consists of micro computed tomography (micro-CT) image of real Earth rock samples with high resolution. We show that lateral gas density gradients can be produced in a straightforward manner leading to substantial non-radial flow.

1. Introduction

Comets are widely assumed to be the least processed remaining bodies from the formation of the Solar System. The Rosetta mission was designed to investigate a comet in detail and understanding sublimation processes, surface characteristics, and coma formation of comet 67P/Churyumov-Gerasimenko (hereafter 67P) was one of the main objectives. After a ten-year cruise, the Rosetta spacecraft reached 67P on 6 August 2014. The spacecraft was orbiting and observing the comet for two years and has provided a large amount of data. The nucleus of 67P consists of two large lobes joined at a “neck” (Sierks et al., 2015).

The Rosetta orbiter housed a suite of eleven instruments along with the Philae lander in order to observe the nucleus and the coma. The millimetre-submillimetre wave instrument, Microwave Instrument for the Rosetta Orbiter (MIRO), supported analysis of the water vapour distribution in the comet’s inner coma (Gulkis et al., 2007). The Rosetta Orbiter Spectrometer for Ion and Neutral Analysis (ROSINA) determined composition and density in situ. The Comet Pressure Sensor (COPS) of ROSINA provides the total gas density (Hässig et al., 2015). Hassig et al. observed heterogeneities in the coma of 67P with large fluctuations using ROSINA data (Kokorev et al) and Marschall et al. modelled the COPS pressure variations with time in the November 2014 period using an inhomogeneous outgassing distribution (Marschall et al., 2017). Similar results were also reported by other studies (Bieler et al., 2015; Fougere

et al., 2016). The Visual InfraRed Thermal Imaging Spectrometer (VIRTIS) instrument made measurements of the coma and showed that the neck of 67P is the region where H₂O mostly emanates during northern summer (Bockelée-Morvan et al., 2015). This was in agreement with the modelling of the COPS data. However, CO₂ emanates from the two lobes (Migliorini et al., 2016). Differences in the outgassing distributions of different species had been seen during flybys of other comets (Feaga et al., 2007).

The inhomogeneities in gas outgassing could arise from variations in the surface layer porous structure. But a non-uniform dust layer composed of particles with varying size could also be realistic scenario (Skorov et al., 2011; Shi et al., 2016). Non-uniform outgassing from the nucleus surface might give rise to the inhomogeneities (Shi et al., 2016). Coma inhomogeneities can also be attributed to non-uniformly distributed sources of H₂O and CO₂ over the surface of the nucleus (Biver et al., 2015).

The Optical Spectroscopic and Infrared Imaging System (OSIRIS) has yielded unprecedented views of 67P. Images have shown that the surface is morphologically complex. Thomas et al. reported the presence of large dune-like ripples on 67P (Thomas et al., 2015a). The presence of such dunes on a comet challenged the existing knowledge and understanding of comet surface processes as it indicated non-radial gas flow. The suggestion that water vapour is emitted from a subsurface ice and travel through a porous medium was considered realistically in a detailed study

* Corresponding author. Heriot-Watt University, Institute of Mechanical Process and Energy Engineering, EH14 4AS, Edinburgh, Scotland, UK.
E-mail address: c.christou@tickmill.com (C. Christou).

(Jia et al., 2017).

The Philae lander contacted the surface of 67P on the northern hemisphere of the nucleus (Biele et al., 2015). The Multipurpose Sensors for Surface and Sub-Surface Science (MUPUS) was designed to measure thermomechanical properties of the surface and the near-surface layer and to monitor the subsurface temperature (Spohn et al., 2015). However, MUPUS was unable to be inserted and thermomechanical properties were not measured. Hammering was increased to the highest energy level but it was not able to be inserted more than 27 mm (Spohn et al., 2015). Spohn et al. interpreted this failure to a near-surface layer of a strength that MUPUS was not capable of penetrating (Spohn et al., 2015). With a data calibration, the uniaxial (or unconfined) compressive strength of the material was calculated to be about 2 MPa. This is at odds with measurements of the tensile and compressive strengths elsewhere and has led to the idea that the surface layer may be locally inhomogeneous in its physical properties. Furthermore, Brouet et al. reported the presence of an upper layer with different physical properties to the interior and suggested the existence of a porosity gradient with increasing porosity with depth (Brouet et al., 2016).

Comets are now known to be highly porous and could have a porosity around 85% (Skorov et al., 2011) or in the range of 75–85% at the “head” (Pätzold et al., 2016). Similar porosity values have also been calculated but with lower boundaries corresponding to a porosity 70–75% (Jorda et al., 2016).

The above observations suggest that inhomogeneity in outgassing is a highly probable property of cometary nuclei, that surface morphology is variable over many scales, and that porosity gradients exist with depth and possibly with lateral position. We expect these properties to influence the near-surface gas flow field. Here we investigate one hypothesis, namely, whether porosity gradients in a surface layer can influence the gas flow from a sublimating sub-surface ice layer. We do this using physical analogues.

We have used micro computed tomography (micro-CT) of terrestrial rock samples to demonstrate some possible rarefied gas flow phenomena. The direct simulation Monte Carlo (DSMC) method is adopted. DSMC has been previously used for simulating the activity around comets and it has been able to reproduce ROSINA observations (Fougere et al., 2016). The porous medium sample consists of porosity between 45 and 92%. In the next section, we discuss the porous material analogues. In section 3, we discuss the model. In section 4, we describe the main results and then conclude.

2. X-Ray Micro computed tomography (micro-CT) images

A typical method to study gas transport in near-surface comet porous layers is to generate porous media with monodisperse spheres using either random ballistic deposition (RBD) or random sequential packing (RSP) (Skorov et al., 2011). While this method can provide us with any targeted porosity it does not represent real porous medium (rock) samples. Feldkamp et al. first reported micro-CT X-Ray technology in 1980's and it was used to study bones (Feldkamp et al., 1989). Micro-CT technology can represent any object with high resolution in three dimensions (3D) and its applications are found in several areas of engineering including medical applications and petroleum industries. Micro-CT allows scientists to analyze the medium in three-dimensions (3D). The method enables a direct measurement of the sample microarchitecture. The explosion of unconventional gas extraction in the oil and gas sectors has boosted micro-CT scan of porous media. The fact that unconventional gas reservoirs consist of low porosity media indicates also the need for high resolution images in this area. Resolutions of micro-CT images are now in the scale of μm and nm (Dong, 2007). Micro-CT is still though a relatively new technique. The high resolution of this method allows us to calculate the porosity of a sample through the reconstructed image. It should be noted that micro-CT is a non-destructive method, hence samples that have been scanned and are used in simulations can be re-evaluated at any time (Ho and Huttmacher, 2006). Fig. 1 shows the

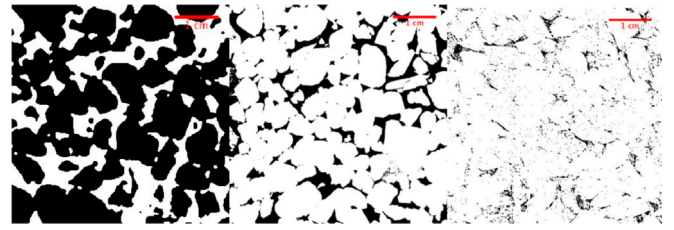


Fig. 1. Binary porosity gradient X-Ray Micro-CT image cross section of porous medium samples used with a resolution of $5\mu\text{m}$. White colour is the material and the black colour is the void area. From left to right ($\phi = 45\%$, $\phi = 80\%$, $\phi = 92\%$).

binary image pore network of three rock types.

Micro-CT technology captures the pore space in detail. Images can then be implemented in an unstructured mesh after the three-dimensional image reconstruction. The capability to use an unstructured mesh directly on the images allows us to use different Computational Fluid Dynamics codes (here the DSMC (Christou and Dadzie, 2016)) to model the fluid flow and extract flow properties through the medium. As DSMC is a discrete method it is convenient for simulating the rarefied gas flow in these complex geometries.

3. Model

Porous structures are complex geometries and networks consisting of pores with different size. Gas flow in porous medium is usually modelled by Darcy's law which is derived from the standard Navier-Stokes equations (Darcy, 1856). Here our outgassing processes through the comet surface from the subsurface are purely rarefied. The degree of rarefaction is characterized by the Knudsen number, Kn (i.e., the ratio of the mean free path, λ , to the characteristic length of porous medium, H)

$$Kn = \lambda/H \quad (1)$$

Fluid flow is often classified into four regimes (Karniadakis et al., 2005): continuum flow ($Kn < 0.001$) in which Navier-Stokes equations are applicable; slip flow regime ($0.001 < Kn < 0.1$) where Navier-Stokes with velocity slip and temperature jump can be used to describe the flow; transition regime ($0.1 < Kn < 10$) and free molecular regime ($Kn > 10$). In the transition and free molecular regimes Navier-Stokes are inapplicable since the flow is far from equilibrium and discrete methods such as DSMC are usually adopted (Chapman and Cowling, 1970). DSMC is a kinetic approach that provides solutions to the Boltzmann equation. Despite its computational demand, DSMC is valid for all collisional regimes encountered in the cometary coma. Depending on the heliocentric distance, the outgassing from the comet surface is found in the transition (close to perihelion) and free molecular (near aphelion) regimes and consequently the gas is in a non-equilibrium state because of the very few intermolecular collisions. In the case where the Knudsen number is greater than unity then the mean free path is higher than the porous media thickness and as a result more collisions with pore walls take place.

Particles are inserted below the porous gradient structure, where we assume the sublimation is taking place. Intermolecular collisions in the current study are treated using the Variable Soft Sphere (VSS) model which has advantages over other models (Shen, 2006). The outer and lateral boundaries are considered to be a vacuum like boundaries. Wall reflection boundaries for the porous media are set to diffuse. For the gas-surface interaction model, diffuse model considered to be more appropriate in comparison with specular model especially for porous media surfaces (Christou and Dadzie, 2016).

Driven by outgassing inhomogeneity observed on 67P, we use Earth basin rock samples of different porosities to construct a porosity gradient geometry. DSMC is applied on the 3D rock images to investigate the outgassing process.

4. A porosity gradient driving flow

We start our investigation by evaluating terrestrial rock samples individually (Fig. 2) in order to illustrate how porosity influences the rarefied flow outgassing pressure. We evaluate six different samples with porosities ranging from 24 to 92% with dimensions of the rock equal to 5cm × 5cm × 5cm. We assume gas emission from the interior with flow through the porous samples to the surface. The gas production rate is $Z = 3 \times 10^{22}$ molecules $\text{m}^{-2} \text{s}^{-1}$ in the interior. Table 1 reports the pressures at the surfaces of the porous rock samples. The surface outgassing pressure ratio between rocks with porosity 92% and 45% is nearly 50. Rock samples with relatively low porosity (24% and 45%) are acting almost as seal rocks; that is, preventing migration of gas molecules to the surface.

From Table 1, we hypothesize that the existence of a lateral porosity gradient along the surface in these rarefaction conditions results in a steep lateral pressure gradient and thus later flow of gas across the surface. We therefore construct a porosity gradient flow configuration combining three rock samples (Fig. 3). Rock samples selected correspond to porosities: 45%, 80% and 92%. The combined three different rock samples represents our non-uniform porous comet structure. Two production/sublimation rates are investigated. The effects of a porosity gradient orthogonal to this, i.e., a porosity increasing or decreasing with depth has previously been investigated (Brouet et al., 2016). Here, we focus on the lateral porosity gradient effects on the flows in the near surface boundary layer assuming water vapour as the outgassing gas. For the DSMC simulations, binary collisions are treated using the variable soft sphere model (VSS). Collisions of gas molecules with the boundaries are assumed to be fully diffusive (Shen, 2006). Such a model has been previously reported to have advantages over a specular reflection model. Each simulation case consists of more than five million computational cells. All cells meet the size criterion, in order to be less than the mean free path (λ). Each computational cell contains approximately thirty particles. The DSMC code implemented in the OpenFOAM framework is used in the current study (Scanlon et al., 2015).

Fig. 3 depicts the configuration under investigation. It is suggested that water ice is present very close (some cm's) below the surface in several places of 67P (Auger et al., 2018). Thus, we use a micro-CT digital rock with total length of 15 cm and a height equal to 5 cm. Sublimation is assumed to take place 5 cm below the surface at a uniform rate and temperature $T_{\text{gas}} = 200\text{K}$. Two gas production rates are assumed, namely, $Z = 3 \times 10^{19}$ & 22 molecules $\text{m}^{-2} \text{s}^{-1}$ (Hansen et al., 2016). The porous

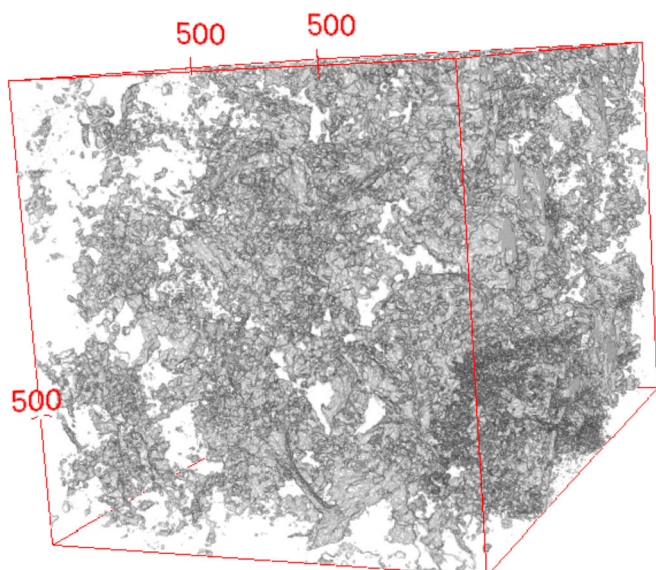


Fig. 2. X-Ray Micro-CT reconstructed 3D digital image sample.

Table 1

Surface gas pressure as a function of porosity for production rate, $Z = 3 \times 10^{22}$ molecules $\text{m}^{-2} \text{s}^{-1}$.

porosity (%)	Pressure ($\text{Pa} \times 10^{-4}$) at the surface
92	150
90	110
88	112
80	54.4
45	3.6
24	3.1

rock sample has a constant temperature $T_{\text{rock}} = 300\text{K}$. Above the surface is considered an open-domain. Next, we look into the flow properties at a distance of few centimeters above the surface, on the Y-axis. This configuration which is on the centimetre scale may be viewed as a pore scale modelling rather than at the full 67P scale. An upscaling method may be used to translate results into the macroscopic or kilometre scale (Valvatne and J.W.r.r. Blunt, 2004). Then gas properties obtained in the few cm's scale above the surface can serve as input in models describing the gas flow in the scale of the km (Liao et al., 2016).

5. Results and discussion

Fig. 4 illustrates the lateral pressure profiles at 1 cm above surface from DSMC simulations data for the two heliocentric distances. High surface pressure is observed at the high porosity side and low at the low porosity side. We observe therefore a steep pressure gradient in the direction of increasing porosity generated by the existence of a lateral porosity gradient despite a constant production rate at source. The outgassing pressure shows a rapid increase with a small change in porous media porosity. In more detail, Fig. 4a and b shows that outgassing pressure can be up to seven times higher by increasing the porosity 47%.

In Fig. 5 we look into the lateral velocity profile in the negative pressure gradient direction corresponding to porosity gradient set-up in the previous section. We observe a lateral velocity of over 550 m/s which expands into the low pressure ron. The fraction of the lateral component to the speed of the gas is 0.85. This indicates that the flow is indeed mainly parallel to the surface. These lateral flow velocities are difficult to compare with Rosetta data but these values are similar to those seen for radial expansion. Gulkis et al. reported from MIRO observations, a radial expansion velocity of 680 m/s which is comparable to the range of lateral velocity obtained in the high porosity ron from our simulations (Gulkis et al., 2015). Lower values than the one reported by Gulkis et al. were reported by Bieler et al. (2015). Biver et al. investigated the expansion velocity for a heliocentric distance of 3.4 au and reported values of 470–590 m/s (Biver et al., 2015). Marschall et al. hypothesized that the red emission wing in the HO line shape of some MIRO spectra could indicate an almost stagnant layer close to the nucleus surface. Due to their observed viewing geometry such a stagnant layer would not imply zero gas velocity but rather a lateral gas flow (Marschall et al., 2019).

On the modelling side, Thomas et al. by assuming a gas number density of $5 \times 10^{16} \text{m}^{-3}$ calculated a shear velocity at a fluid threshold for $d = 1$ cm diameter particles that gave 528 m/s and concluded that particles of that size and larger might be lifted by such a flow (Thomas et al., 2015b). The gas pressure used in that study was comparable to the one used in our DSMC simulations. It is worth noting that shear velocity at velocity threshold is proportional to gas pressure. Recently Jia et al. compared bedforms observed on 67P to giant ripples (Pätzold et al., 2016).

In the case where the production rate is equal to $Z = 3 \times 10^{19}$ molecules $\text{m}^{-2} \text{s}^{-1}$ the gas is more rarefied and the Knudsen number is three orders of magnitudes higher. Hence, the outgassing flow is far from equilibrium and there are more collisions between gas molecules and boundaries than intermolecular collisions. Porosity gradient flows occurs in both reported production rates (Fig. 5) however the velocity is lower for the higher Knudsen number (low production rate).

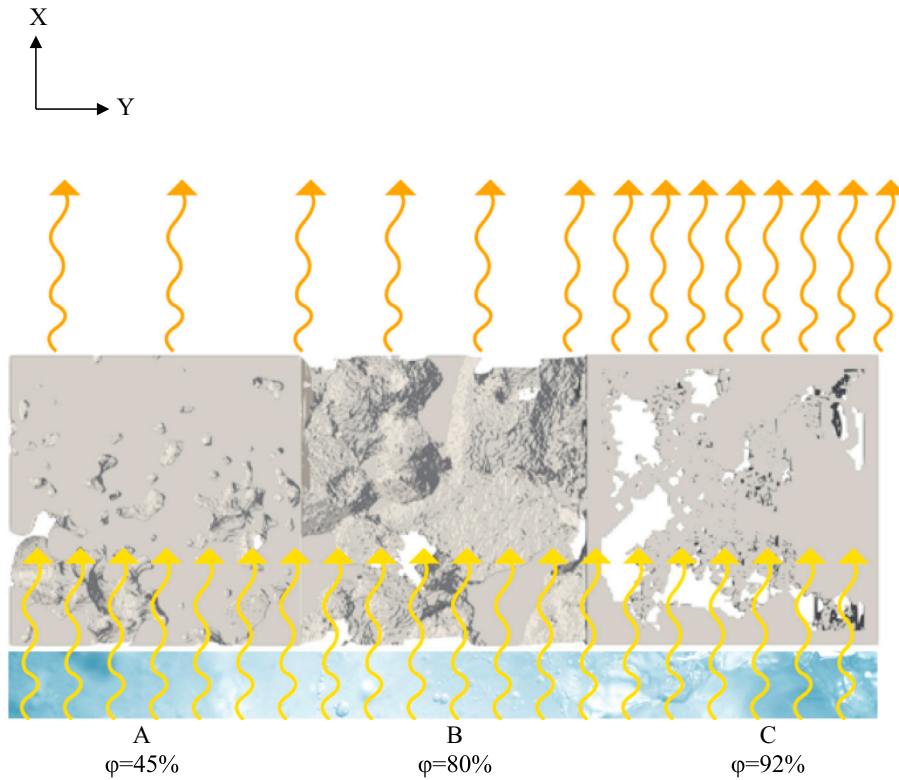


Fig. 3. Problem configuration (porosity gradient structure). Rock temperature, $T_{\text{rock}} = 300\text{K}$ and gas sublimation temperature $T_{\text{gas}} = 200\text{K}$.

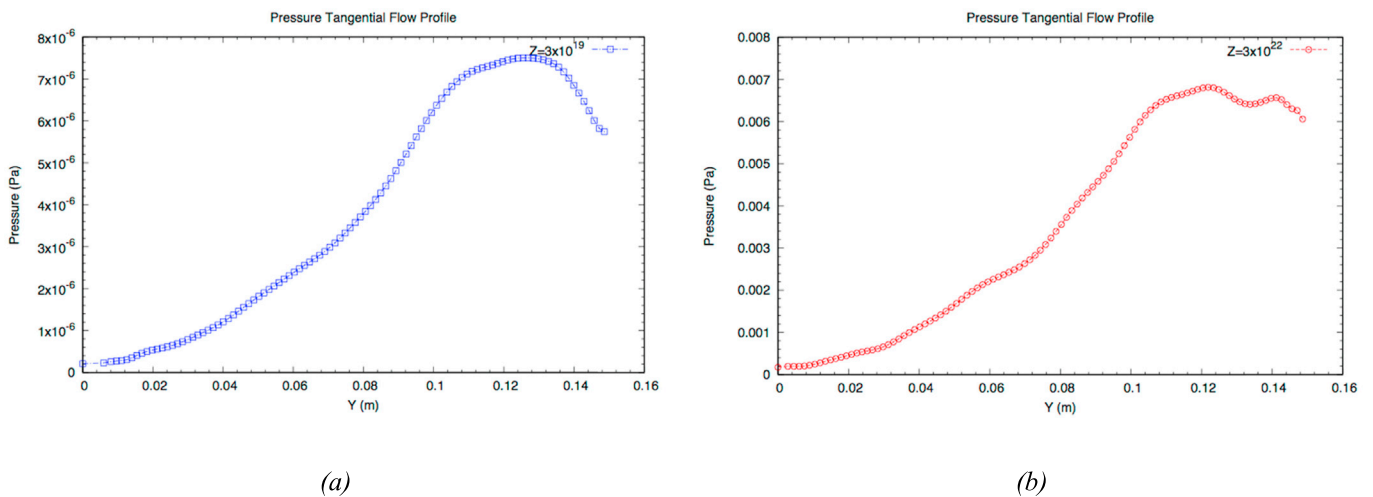


Fig. 4. Outgassing pressure profiles for two different production rates at 1 cm above surface. a) $Z = 3 \times 10^{19}$ and b) $Z = 3 \times 10^{22}$.

Comparing Figs. 4 and 5 we observe a positive correlation between pressure and velocity profiles. Such observations confirm some previous reports (Davidsson et al., 2010). Fig. 6 presents the temperature profile corresponding to the porosity gradient driving flow configuration. The non-uniformity in the comet near surface porous media layer results in lateral temperature gradients. The outgassing gas temperature at the surface decreases as the porosity increases. That is, the gas temperature at the surface is inversely proportional to porosity. On average, 170 K is the minimum gas surface temperature obtained with the higher porosity medium. The highest temperature is found for a medium with porosity of 45% which is on average 215 K (Christou et al., 2018). In other words, the temperature jump at the nucleus surface increases with porosity. Taking into account this temperature gradient it may be concluded that

the higher speed flow depicted in Fig. 5 is a combination of both temperature and pressure gradient effects.

These lateral flows may be capable of generating grain transports. Lara et al. reported that dust particles in the scale of mm could be ejected (Lara et al., 2015). More recently, Lia et al. calculated that during peak production, near perihelion passage, dust grains can be as large as up to 10 mm when ejected from the nucleus surface (Lai et al., 2017). Based on those observations and the lateral velocity in Fig. 5 we can conclude that porosity gradient can generate the transport of grains that are ejected from the surface.

Lee et al. reported that outgassing activity can be affected by many local environmental factors such as: the present amount of water ice, porosity layer and surface temperature (Lee et al., 2015). The current

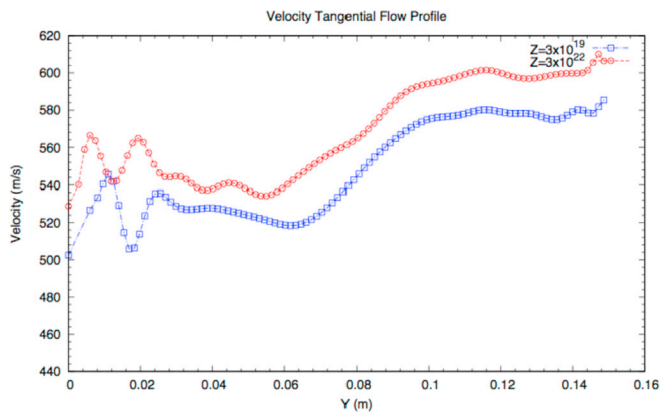


Fig. 5. Outgassing lateral velocity profiles for two different production rates.

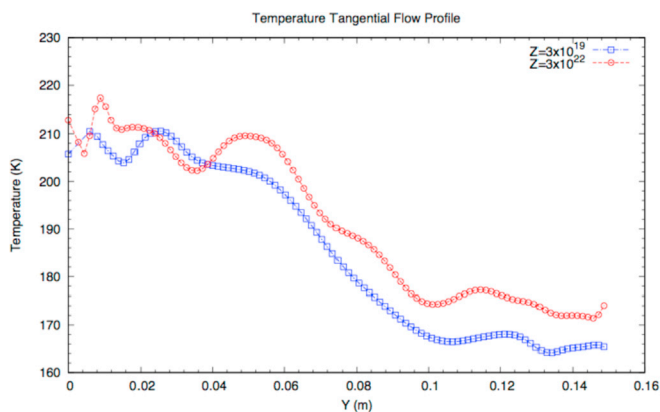


Fig. 6. Outgassing temperature above surface for porosity gradient; lower porosity on the left side and higher on the right.

work directly depicts the porosity layer and surface temperature factors. Starting from porosity of the medium in the near-surface non-equilibrium outgassing activity it has been shown that it can be affected by porosity variations and interestingly it can be driven by it. Such flows can also be found in both the active and inactive rons. However, inactive rons are with higher Knudsen number flows and hence with more rarefied conditions (Hässig et al., 2015). Fig. 4 indicates that the present porosity gradient flows may be observed in both rons.

6. Concluding remark

We have presented numerical simulations of gas dynamics within the first few centimetres of comet-like surface layers. We demonstrate how a lateral porosity gradient can generate steep lateral pressure and temperature gradients leading to potentially high speed lateral flows. This follows observations of sediment transports at the surface of comet 67P. These results add a new perspective to the observed inhomogeneities in coma formation. Previously lateral surface flows leading to dune-like structures observed on 67P were explained by temperature differences between highly illuminated and shadowed rons on the nucleus. Our present results indicate that porosity variations by themselves may be responsible for lateral flows and we suggest that these may be capable of generating substantial grain transports. We also observed that a difference in porosity creates a large difference in the difference between gas and comet material temperature at the surface (i.e., in the surface temperature jump).

We found that even small variations in porosity (12%) result in significant changes in outgassing properties. For the reported observations at a distance of a few centimetres above the surface medium, an increase

in porosity, results in an increase in surface water vapour pressure. Summarizing, we propose that a structure with varying porosity that might be present in different rons of the comet's surface could also contribute to the observed coma inhomogeneities. We conclude that the coma might have an additional non-time-dependent component which is related to lateral porosity gradients.

Acknowledgments

This project has received funding from the European Union's Horizon2020 Research and Innovation programme under grant agreement No 686709 (MiARD). This work was supported by the Swiss State Secretariat for Education, Research and Innovation (SERI) under contract number 16.0008–2. The opinions expressed and arguments employed herein do not necessarily reflect the official view of the Swiss Government. The authors would also like to thank iRockTechnologies, Beijing, China, for providing us with the Earth rock samples.

References

- Auger, A.-T., et al., 2018. Meter-scale thermal contraction crack polygons on the nucleus of comet 67P/Churyumov-Gerasimenko. *Icarus* 301, 173–188.
- Biele, J., et al., 2015. The landing (s) of Philae and inferences about comet surface mechanical properties. *Science* 349 (6247), aaa9816.
- Bieler, A., et al., 2015. Comparison of 3D kinetic and hydrodynamic models to ROSINA-COPS measurements of the neutral coma of 67P/Churyumov-Gerasimenko. *Astron. Astrophys.* 583, A7.
- Biver, N., et al., 2015. Distribution of water around the nucleus of comet 67P/Churyumov-Gerasimenko at 3.4 AU from the Sun as seen by the MIRO instrument on Rosetta. *Astron. Astrophys.* 583, A3.
- Bockelée-Morvan, D., et al., 2015. First observations of H₂O and CO₂ vapor in comet 67P/Churyumov-Gerasimenko made by VIRTIS onboard Rosetta. *Astron. Astrophys.* 583, A6.
- Brouet, Y., et al., 2016. A porosity gradient in 67P/CG nucleus suggested from CONSERT and SESAME-PP results: an interpretation based on new laboratory permittivity measurements of porous icy analogues. *Mon. Not. R. Astron. Soc.* 462 (Suppl. 1_1), S89–S98.
- Chapman, S., Cowling, T.G., 1970. *The Mathematical Theory of Non-uniform Gases: an Account of the Kinetic Theory of Viscosity, Thermal Conduction and Diffusion in Gases*. Cambridge university press.
- Christou, C., et al., 2018. Gas flow in near surface comet like porous structures: application to 67P/Churyumov-Gerasimenko. *Planet. Space Sci.* 161, 57–67.
- Christou, C., Dadzie, S.K., 2016. Direct-simulation Monte Carlo investigation of a berea porous structure. *SPE J.* 21 (3), 938–946.
- Darcy, H., 1856. *Les fontaines publiques de la ville de Dijon: exposition et application*. Victor Dalmont.
- Davidsson, B.J., et al., 2010. Gas kinetics and dust dynamics in low-density comet comae. *Icarus* 210 (1), 455–471.
- Dong, H., 2007. *Micro-CT Imaging and Pore Network Extraction*.
- Feaga, L., et al., 2007. Asymmetries in the distribution of H₂O and CO₂ in the inner coma of Comet 9P/Tempel 1 as observed by deep impact. *Icarus* 191 (2), 134–145.
- Feldkamp, L.A., et al., 1989. The direct examination of three-dimensional bone architecture in vitro by computed tomography. *J. Bone Miner. Res.* 4 (1), 3–11.
- Fougere, N., et al., 2016. Three-dimensional direct simulation Monte-Carlo modeling of the coma of comet 67P/Churyumov-Gerasimenko observed by the VIRTIS and ROSINA instruments on board Rosetta. *Astron. Astrophys.* 588, A134.
- Gulkis, S., et al., 2007. MIRO: Microwave instrument for Rosetta orbiter. *Space Sci. Rev.* 128 (1–4), 561–597.
- Gulkis, S., et al., 2015. Subsurface properties and early activity of comet 67P/Churyumov-Gerasimenko. *Science* 347 (6220), aaa0709.
- Hansen, K.C., et al., 2016. Evolution of water production of 67P/Churyumov-Gerasimenko: an empirical model and a multi-instrument study. *Mon. Not. R. Astron. Soc.* 462 (Suppl. 1_1), S491–S506.
- Hässig, M., et al., 2015. Time variability and heterogeneity in the coma of 67P/Churyumov-Gerasimenko. *Science* 347 (6220), aaa0276.
- Ho, S.T., Hutmacher, D.W., 2006. A comparison of micro CT with other techniques used in the characterization of Scaffolds. *Biomaterials* 27 (8), 1362–1376.
- Jia, P., Andreotti, B., Claudin, P., 2017. Giant ripples on comet 67P/Churyumov-Gerasimenko sculpted by sunset thermal wind. In: *Proceedings of the National Academy of Sciences*, p. 201612176.
- Jorda, L., et al., 2016. The global shape, density and rotation of Comet 67P/Churyumov-Gerasimenko from preperihelion Rosetta/OSIRIS observations. *Icarus* 277, 257–278.
- Karniadakis, G., Beşkök, A., Aluru, N.R., 2005. *Microflows and Nanoflows: Fundamentals and Simulation*. Interdisciplinary Applied Mathematics. Springer, New York, NY, p. 817 xxi.
- Kokorev, V.I., et al., The Impact of Thermogas Technologies on the Bazhenov Formation Studies Results. *Society of Petroleum Engineers*.
- Lai, I.-L., et al., 2017. Gas Outflow and Dust Transport of Comet 67P/Churyumov-Gerasimenko, 462, pp. S533–S546. Suppl. 1_1.

- Lara, L., et al., 2015. Large-scale Dust Jets in the Coma of 67P/Churyumov-Gerasimenko as Seen by the OSIRIS Instrument Onboard Rosetta, vol. 583, p. A9.
- Lee, S., et al., 2015. Spatial and diurnal variation of water outgassing on comet 67P/Churyumov-Gerasimenko observed from Rosetta/MIRO in August 2014. *Astron. Astrophys.* 583, A5.
- Liao, Y., et al., 2016. 3D Direct Simulation Monte Carlo modelling of the inner gas coma of comet 67P/Churyumov-Gerasimenko: a parameter study. *Earth Moon Planets* 117 (1), 41–64.
- Marschall, R., et al., 2017. Cliffs versus Plains: Can ROSINA/COPS and OSIRIS Data of Comet 67P/Churyumov-Gerasimenko in Autumn 2014 Constrain Inhomogeneous Outgassing?.
- Marschall, R., et al., 2019. A comparison of multiple Rosetta data sets and 3D model calculations of 67P/Churyumov-Gerasimenko coma around equinox (May 2015). *Icarus* 328, 104–126.
- Migliorini, A., et al., 2016. Water and carbon dioxide distribution in the 67P/Churyumov-Gerasimenko coma from VIRTIS-M infrared observations. *Astron. Astrophys.* 589, A45.
- Pätzold, M., et al., 2016. A homogeneous nucleus for comet 67P/Churyumov-Gerasimenko from its gravity field. *Nature* 530 (7588), 63–65.
- Scanlon, T., et al., 2015. Open-source direct simulation monte carlo chemistry modeling for hypersonic flows. *AIAA J.* 53 (6), 1670–1680.
- Shen, C., 2006. *Rarefied Gas Dynamics: Fundamentals, Simulations and Micro Flows*. Springer.
- Shi, X., et al., 2016. Sunset jets observed on comet 67P/Churyumov-Gerasimenko sustained by subsurface thermal lag. *Astron. Astrophys.* 586, A7.
- Sierks, H., et al., 2015. On the nucleus structure and activity of comet 67P/Churyumov-Gerasimenko. *Science* 347 (6220), aaa1044.
- Skorov, Y.V., et al., 2011. Activity of comets: gas transport in the near-surface porous layers of a cometary nucleus. *Icarus* 212 (2), 867–876.
- Spohn, T., et al., 2015. Thermal and mechanical properties of the near-surface layers of comet 67P/Churyumov-Gerasimenko. *Science* 349 (6247), aab0464.
- Thomas, N., et al., 2015. The morphological diversity of comet 67P/Churyumov-Gerasimenko. *Science* 347 (6220), aaa0440.
- Thomas, N., et al., 2015. Redistribution of particles across the nucleus of comet 67P/Churyumov-Gerasimenko. *Astron. Astrophys.* 583, A17.
- Valvatne, P.H., J.W.r.r. Blunt, M.J., 2004. *Predictive Pore-scale Modeling of Two-phase Flow in Mixed Wet Media*, vol. 40, 7.